Article

JOURNAL OF THE CHINESE CHEMICAL SOCIETY

Field Emission and Superhydrophobic Properties of Electrochemically Grown Gold Nanourchins

Ting-Kai Huang,[a] Hsin-Wei Huang,[a] Chi-Young Lee[b] and Hsin-Tien Chiu[a,*]

[a]*Department of Applied Chemistry, National Chiao Tung University, Hsinchu, Taiwan, 30050, R.O.C.*

[b]*Department of Materials Science and Engineering and Center for Nanotechnology, Materials Science, and Microsystems, National Tsing Hua University, Hsinchu, Taiwan, 30043, R.O.C.*

(Received: Oct. 17, 2011; Accepted: Apr. 3, 2012; Published Online: May 29, 2012; DOI: 10.1002/jccs.201100611)

We demonstrate a convenient fabrication of Au nanourchins (NUs) on Si substrates via a surfactant-assisted galvanic reduction process. This synthetic method not only grows Au NUs on Si in a one-step process but also effectively controls the lengths of the branches on the NUs. The widths are about 100-120 nm and the lengths can be extended from 200 nm to 5 μm by lengthening the growth time. With the advantage of a hierarchical surface structure, Au NUs exhibited excellent electron field emission (FE) performance (turn-on voltage, 6.3 V/μm; β, 1150). In addition, the wetting behavior examination shows that the water contact angle can be as high as 158° on Au NUs after the material is treated by 1-hexadecanethiol.

Keywords: Gold; Nanourchin; Galvanic reduction; Electron field emission; Superhydrophobicity.

INTRODUCTION

Gold nanourchins (NUs), composed of a central nanocore and several protruding tips, have been attracting research interests, due to their potential applications in molecular detections[1,2] biosensing,[3,4] and immunoassay.[5,6] The nanostructure has been alternatively named as nanoflowers,[7] nanostars[8] and multi-branched nanoparticles (NPs).[9-11] Similar to other anisotropic NPs, such as nanorods, nanosheets, and nanocubes, they exhibit strong electromagnetic field enhancement capability upon irradiation.[12] Therefore, they are important for surface enhanced Raman scattering (SERS) spectroscopy and imaging.[1,13,14] Although electron field emission (FE) properties of metallic nanowire (NW) arrays have been reported,[15-19] we are unable to find similar investigations on NUs. Compared with semiconductor FE arrays, metallic NW arrays, such as Cu NWs and Au NWs, may generate efficient electron emissions due to their low resistivity, low work function, and high refractivity.[15-21] On the other hand, anisotropic metallic nanomaterials with high surface roughness and potential for surface modifications have been demonstrated to form superhydrophobic surfaces.[22-27] The property has various applications, such as self-cleaning paint and antiwetting fabrics.[28-34] Recently, we reported the growth of Au NWs on Si.[35] In this study, we discover that by proper control of the reaction conditions, Au NUs could be obtained. The synthetic method, that avoids hard templates, expensive instruments, and complicated processing, is relatively facile compared with the conventional approach to fabricate multi-tips on surfaces.[15-27] Therefore, the refined experiments associated with the morphological control and length modulation of branches on Au NUs are presented. The as-prepared hierarchical NUs have dense, sharp branches and good electrical contact with Si. These provide potentials for electron FE and superhydrophobic surface applications. Our discoveries will be discussed below.

RESULTS AND DISCUSSION

Recently, we reported a simple method which combined the growth and immobilization of high-aspect-ratio Au NWs in large scale on preroughened Si substrates (an example can be seen in Figure S1 in the supporting information) in a one-step process.[35] The reaction was a galvanic reduction of $HAuCl_{4(aq)}$ by $Sn_{(s)}$ attached to the substrate (Figure S2 in the supporting information) in the presence of $CTAC_{(aq)}$ and $NaNO_{3(aq)}$. We suggested that both CTAC molecules and NO_3^- ions were essential ingredients to shape the highly symmetric fcc Au crystals into the 1D morphology.

Therefore, we adjusted the experimental conditions by shortening the reaction time. This controlled the length of the NWs effectively. Au NUs were obtained. Basically, the NUs were branches extended from central cores (Figure S3 in the supporting information). In order to clarify the effects on the growth conditions, NO_3^- ions and CTAC molecules were not added in some reactions. In these cases, Au

* Corresponding author. E-mail: htchiu@faculty.nctu.edu.tw

microparticles and nanothorns were obtained respectively. The growth parameters for each product are summarized in Table 1.

Characterization of nanostructures

Figure 1 shows the low and high magnification scanning electron microscopic (SEM) images of the Au NUs on Si substrates at various stages of the growth. After grown for 6 h, flower shaped clusters are formed (Figure 1A). The surface coverage of the nanoflowers were presented in Figure S4 in the supporting information. The size of each cluster is estimated to be about 2 μm in diameter. An enlarged view (Figure 1B) shows lots of short spurs less than 200 nm long protruding from the core. The image in Figure 1C reveals the morphology of the clusters after 12 h. They maintain similar coverage on the substrate with no apparent change in their dimensions. However, a detailed image in Figure 2D displays that rod-like nanobranches form and protrude radially. This differs from the image shown in Figure 1B. The diameter and the length of the branches are about 100 nm and up to 300 nm, respectively. After 18 h, densely covered straight Au NWs with diameters 100-120 nm and lengths up to 5 μm extended radially from the core, as shown in the NU shaped structures in Figure 1E. Figure 1F shows a side-view image of a NU on the substrate, with the NWs growing upward in a hemispherical arrangement. The bottom of the NU is located on a cavity of the pre-roughened Si surface apparently. This may correspond to the initial nucleation stage. Figure 2 shows a couple Au branches with tips constructed from pentagonal shaped surface steps. This observation suggests that these branches

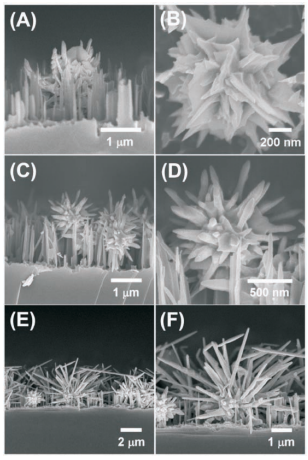

Fig. 1. Side and top view SEM images of Au NUs grown on pre-roughened Si at different growth time. (A) and (B) 6 h. (C) and (D) 12 h. (E) and (F) 18 h.

Table 1. Summary of growth conditions of Au nanostructures.

Sample	$HAuCl_4$ (mM)	CTAC (mM)	$NaNO_3$ (mM)	Time (h)	Temperature (K)
Urchin-6h	5	9	20	6	303
Urchin-12h	5	9	20	12	303
Urchin-12h	5	9	20	18	303
Urchin-27h	5	9	20	27	303
Microparticle	5	9	0	18	303
Nanothorn	5	0	20	18	303

may have a penta-twinned crystal structure, as demonstrated in previous studies.[35-38]

An XRD pattern of the NUs grown on Si is shown in Figure 3. The peaks at $2\theta = 38.1^{o}$, 44.3^{o}, and 64.5^{o} are assigned to Au (111), (200), and (220) reflections, respectively (JCPDF 89-3697). Lattice constant *a* is estimated to be 0.408 nm, close to the reported value of Au, 0.4079 nm (JCPDF 89-3697). The XRD study confirms that the NUs have an fcc structure.

When the growth time was extended to 27 h, ultra long Au NWs were densely covered on the Si substrate. This agreed with our previous report.[35] The diameter and the length were 100 nm and up to 10 μm, respectively. In some areas with low Au NW coverage, the NU structures could still be found.

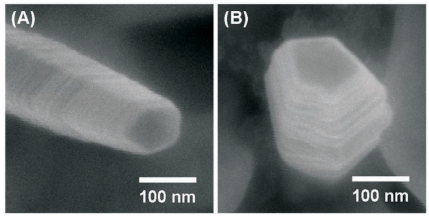

Fig. 2. High magnification SEM images of Au branches on NUs showing tips constructed from pentagonal shaped surface steps.

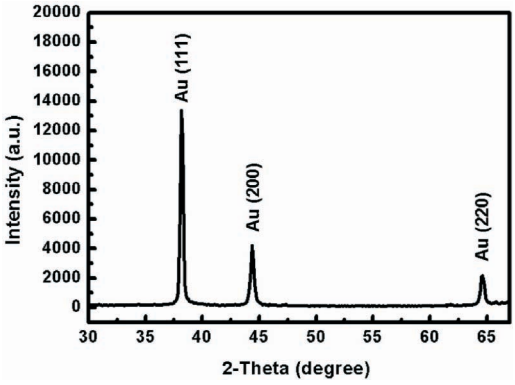

Fig. 3. XRD of Au nanourchin grown on Si.

The presence of adequate amounts of both CTAC molecules and NO_3^- ions played a crucial role in the growth of the NUs. Without NO_3^-, micro-sized particles (diameter 1 μm) were deposited on the Si substrate, as shown in Figure S5 in the supporting information. Most particles grew isotropically and fused together on the substrate. Individual stand-along particles were few. Compared to the NUs, the microparticles had smooth surfaces. In the absence of CTAC, nanothorns were obtained. Figure S6 revealed that each of the Au NTs had a height 1-2 μm, a side width 300-500 nm at the bottom, and a tip about 20 nm at the apex. Apparently, different growth conditions provided different crystal structures in the products.

Field emission properties

With lots of rigid and straight branches pointing outward on the Si substrate, Au NUs may show interesting FE properties. The investigations were conducted in the home-made vacuum chamber with a base pressure 1×10^{-6} torr at the room temperature. The FE properties and the corresponding Fowler-Nordheim (F-N) plot are illustrated in Figure 4A and B, respectively. The turn-on field E_0 is designated as the interceptions of the straight lines extrapolated from the low-field and the high-field segments of the F-N plots. Samples **Nanothorn**, **Urchin-12h**, and **Urchin-18h** show E_0 of 13.3, 10.2, and 6.3 μm^{-1}, respectively. Above this field strength, the emission current densities increase dramatically. Plots of $\ln(J/E^2)$ versus 1/E show straight lines in the high fields. These indicates that the field emission characters follow the model described by Fowler-Nordheim (FN) equation $J = A(\beta^2E^2/\Phi)\exp(-B\Phi^{3/2}/\beta E)$.[39] In the equation, in addition to J and E mentioned above, Φ is the work function of Au (5.00 eV), while A and B are constants, 1.56×10^{-10} (A V^{-2} eV) and 6.83×10^3 (V $eV^{-3/2}$ μm^{-1}), respectively.[16] β is the field enhancement factor, a general index which depends on geometry and morphology of the nanostructure, crystal structure of the material, and density of the emitting points. Here, β values of **Nanothorn**, **Urchin-12h**, and **Urchin-18h** are calculated to be 410, 822, and 1150. In contrast, **Urchin-6h** does not show significant J within the E applied. Obviously, the FE performance correlates strongly with the anisotropic surface nanostructures. The NUs display better electron FE performances than the nanothorns do. In addition, with increasing lengths of the NU branches, the enhancement efficiencies improve as well. The improved ? appears to be from the positively enhanced local electrical field created by the increase in the ratio of length to radius. In addition, compared to the electron FE performances of the metal nanostructures reported in literature, as shown in Table 2, β of Au **Urchin-18h** is superior to most of the other 1D Au and Cu nanostructures.[15-18,40,41]

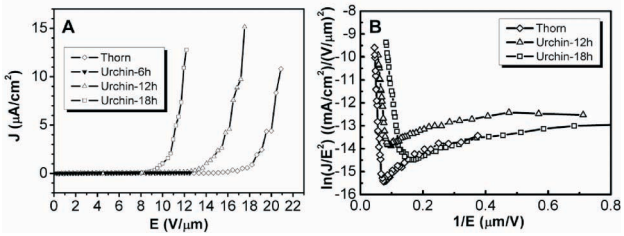

Fig. 4. (A) Emission current density as a function of applied electric field on Au nanostructures. (B) Corresponding Fowler-Nordheim plots.

Contact angle measurements

In the experiments, a measured amount of H_2O (5 μL) was dropped on the surfaces of various Au samples with and without 1-hexadecanethiol treatments. Their corresponding contact angles at the H_2O/Au interface are measured from the images shown in Figure 5. Figure 5A and B show that the contact angles on a flat Au sputtered film increase slightly from 88° to 106° after the surface modifications. Figure 5C-F suggest that even after the surface modifications, the contact angles from the microparticles and the nanothorns do not improve much from the small values. In these cases, both Au nanostructures did not cover the Si substrates below completely, as shown in the SEM images. We suggest that the exposed silicon oxide layer still con-

Table 2. Comparison of electron field emission performance of metal nanostructures

Materials	Fabrication Method	E_0 (V/μm)	β	Reference
Au **Urchin-18h**	Galvanic reduction	6.3	1150	This study
Au **Urchin-12h**	Galvanic reduction	10.2	822	This study
Au **Nanothorn**	Galvanic reduction	13.3	410	This study
Au NWs	ITM[a]/ECD[b]	9	632	16
Cu dendrites	ECD[b]	7.5	1094	40
Cu nanopillars	Galvanic reduction	12.4	713	41
Cu NWs	CVD[c]	4.62	443	15
Cu nanobats	CVD[c]	4	3900	19
Cu NWs	ITM[a]/ECD[b]	6	245	17
Cu NWs	AAO[d]/ECD[b]	44	400	18

[a] ion-track membrane; [b] electrochemical deposition; [c] chemical vapor deposition; [d] anodic aluminum oxide.

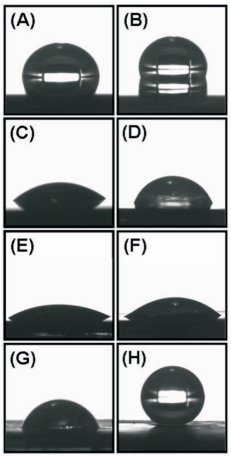

Fig. 5. Contact angle measurements on different Au nanostructures. Sputtered Au film, (A) original and (B) 1-hexadecanethiol modified surface; Au microparticles, (C) original and (D) 1-hexadecanethiol modified surface; Au nanothorns, (E) original and (F) 1-hexadecanethiol modified surface; Au NUs, (G) original and (H) 1-hexadecanethiol modified surface.

tacted the water droplet effectively. These probably resulted in the observed hydrophilic surfaces. Figure 5G shows the contact angle, 71°, of the sample with original NUs. After the surface modification by 1-hexadecanethiol, the contact angle increases significantly to 158° (Figure 5H). According to Cassie equation, $\cos\theta_r = f_1\cos\theta_1 - f_2$, roughening a surface would increase the apparent water/surface contact angle θ_r.[42] θ_1 is the contact angle from the smooth surface without the roughening. f_1 is the fractional interfacial area between the water droplet and the roughened surface while f_2 is the remaining area from the water/air interface. The sum of f_1 and f_2 equals 1. Based on the equation alone, θ_r should not vary significantly for the samples shown in Figure 5G and H because the surface morphology did not change before and after the 1-hexadecanethiol treatment. Thus, the observed contact angle difference is attributed to the different properties of the molecules covering the Au surface. The original NU sample was covered by CTAC, the residual surfactant molecules which assisted the nanostructure growth and adsorbed on the Au surface. This caused the sample to be more hydrophobic than it was expected and to display a small θ_r, 71°. After the 1-hexadecanethiol treatment, the CTAC molecules adsorbed on the Au surface were replaced by the hydrophobic thiol molecules with aliphatic hydrocarbon chains. Consequently, the contact angle increased to 158°. Here, f_2 is estimated to be 0.89. Based on f_2, it is proposed that a high fraction of air was generated on the surface after the surface of the Au NUs was changed from hydrophilic to hydrophobic.[28-30] The modification of the surface property provided the superhydrophobic behavior. The superhydrophobic performance of the Au NUs is comparable to the results reported recently for many anisotropically structured nanometals, such as nanosized cauliflower-like Au, NW arrays of Cu, Pt and Ni, and nanodendrites of Ag.[22-27] They displayed contact angles 153°-174°, after various hydrophobic surface treatments.

CONCLUSION

In conclusion, Au NUs can be grown directly on Si through a surfactant-assisted electrochemical method. Each NU comprises dense and straight NWs that expend outward from the core. Their lengths increase with increasing the growth time. FE measurements show that the nanourchins grown for 18 h emit electrons under relatively low electric field strength and show high β values compared to the other Au and Cu nanostructures reported in literature. The Au NUs surface modified with 1-hexadecanethiol lead to the formation of a superhydrophobic surface. We anticipate that the nanourchin structure could be employed for various FE and anti-wetting applications in the future.

EXPERIMENTAL

Pre-treatment of silicon substrate

A n-type Si (100) wafer (TSR High Purity Si) was pre-roughened by an electroless etching process for facilitating Au nucleation in the process of growing Au nanostructures. After cleaned with acetone, the Si substrate, cut into 0.5 cm × 0.5 cm in size, was immersed into a Teflon bottle containing an etching solution, which was a mixture of $AgNO_3$ (0.07 g, Fisher), HF (48% w.t., 2 mL, Merck) and deionized water (10 mL) for 5 min. After the etching step, the substrate was washed with concentrated HNO_3 (J. T. Baker) and followed by deionized water to remove Ag precipitates formed in the etching process. Finally, the pre-roughened Si was dried under a N_2 stream.

Fabrication of Sn-pasted silicon

A piece of Sn metal (1 mm × 1 mm, Aldrich), used as the reducing metal, was pasted on the backside of the pre-roughened Si substrate by conductive Ag glue (Toyobo). Then, the combined piece was dried in the oven at 383 K for 1 h. Figure S2 in the supporting information displayed its cartoon configuration.

Growth of Au nanourchins

In a glass vial, a mixed growth solution containing $HAuCl_{4(aq)}$ (5 mM, SHOWA), $CTAC_{(aq)}$ (9 mM, Taiwan Surfactant) and $NaNO_{3(aq)}$ (20 mM, Shimakyu's Pure Chemicals) was prepared. It turned yellowish cloudy after mixing. Then, the Sn-pasted Si was immersed into the growth solution (4 mL), maintained at 303 K without stirring during reaction process. The growth time was properly controlled (6, 12, 18 and 27 h), so that the morphology evolution can be observed as the function of time. Gradually, the solution near the wafer turned pink and the Si surface became golden. The final sample specimen was removed from the solution, rinsed with deionized water, and then dried under a N_2 stream before further investigations.

Additionally, microparticles and nanothorns were also prepared using the same electrochemical method. The only difference was the absence of $NaNO_3$ or CTAC in the reaction solution. The concentration of each component and the growth condition are summarized in Table 1.

Instruments for characterization

The SEM images and the energy dispersive spectroscopic (EDS) data were taken from a Hitachi S-4000 (25 keV) and a JEOL JSM-7401F (15 keV). X-ray diffraction (XRD) data were obtained from a Bruker AXS D8 Advance.

Electron field emission measurement

The electron FE properties of the samples were measured in a home-made instrument with a vacuum chamber (base pressure 1×10^{-6} torr) at the room temperature. A stainless-steel probe (diameter 1 mm) was used as the anode. The sample-to-anode distance was adjusted properly by a micrometer on the manipulator. The current-voltage (I-V) characteristics were measured using a Keithley 2410. A positive voltage sweep up to 1 kV with a step of 50 V was applied to the anode.

Wettability measurement

For a typical preparation of superhydrophobic surface, the samples were immersed in an alcohol solution containing 1-hexadecanethiol (2 mM, Alfa Aesar) for 24 hours. After that, the samples were cleaned with alcohol and dried under a N_2 stream.

The contact angles of the samples before and after the surface modification were acquired using a KRUSS universal surface tester (model GH-100). A designated amount of water (5 μl) was dropped on the samples for measurements.

ACKNOWLEDGEMENTS

We are thankful for support from the National Science Council, "Aim for the Top University Plan" of the National Chiao Tung University, and the Ministry of Education of Taiwan, Republic of China.

REFERENCES

1. Esenturk, E. N.; Walker, A. R. H. *J. Raman Spectrosc.* **2009**, *40*, 86.
2. Aaron, J.; Rosa, E. de la; Harrison, K. N.; Burt, J.; Yacaman, M. J.; Sokolov, K. *Opt. Express* **2008** *16*, 2153.
3. Dondapati, S. K.; Sau, T. K.; Hrelescu, C.; Klar, T. A.; Stefani, F. D.; Feldmann, J. *ACS Nano* **2010**, *4*, 6318.
4. Hutter, E.; Boridy, S.; Labrecque, S.; Lalancette-Hebert, L.; Kriz, J.; Winnik, F. M.; Maysinger, D. *ACS Nano* **2010**, *4*, 2595.
5. Wang, S.; Wu, Z.; Qu, F.; Zhang, S.; Shen, G.; Yu, R. *Biosens. Bioelectron.* **2008**, *24*, 1020.
6. Wang, Z.; Zhang, J.; Ekman, J. M.; Kenis, P. J. A.; Lu, Y. *Nano Lett.* **2010**, *10*, 1886.
7. Xie, J. P.; Zhang, Z. Q.; Lee, J. Y.; Wang, D. I. C. *ACS Nano* **2008**, *2*, 2473.
8. Kumar, P. S.; Pastoriza-Santos, I.; Rodriguez-Gonzalez, B.; Garciade de Abajo, F. J.; Liz-Marzan L. M. *Nanotechnology* **2008**, *19*, 015606.
9. Bakr, O. M.; Wunsch, B. H.; Stellacci, F. *Chem. Mater.* **2006**, *18*, 3297.
10. Xie, J. P.; Lee, J. Y.; Wang, D. I. C. *Chem. Mater.* **2007**, *19*, 2823.
11. Maiorano, G.; Rizzello, L.; Malvindi, M. A.; Shankar, S. S.; Martiradonna, L.; Falqui, A.; Cingolani, R.; Pompa, P. P. *Nanoscale* **2011**, *3*, 2227.
12. Nehl, C. L.; Liao, H.; Hafner, J. H. *Nano Lett.* **2006**, *6*, 683.
13. Khoury, C. G.; Vo-Dinh, T. J. *J. Phys. Chem. C* **2008**, *112*, 18849.
14. Rodriguez-Lorenzo, L.; Alvarez-Puebla, R. A.; Abajo, F. J. G.; Liz-Marzan, L. M. *J. Phys. Chem. C* **2010**, *114*, 7336.
15. Kim, C.; Gu, W. H.; Briceno, M.; Robertson, I. M.; Choi, H.; Kim, K. *Adv. Mater.* **2008**, *999*, 1.
16. Dangwal, A.; Pandey, C. S.; Muller, G.; Karim, S.; Cornelius, T. W.; Trautmann, C. *Appl. Phys. Lett.* **2008**, *92*, 063115.
17. Maurer, F.; Dangwal, A.; Lysenkov, D.; Muller, G.; Toimil-Molares, M. E.; Trautmann, C.; Brotz, J.; Fuess, H. *Nucl. Instrum. Methods Phys. Res., Sect. B.* **2006**, *245*, 337.
18. Davydov, D. N.; Sattari, P. A.; AlMawlawi, D.; Osika, A.; Haslett, T. L.; Moskovits, M. *J. Appl. Phys.* **1999**, *86*, 3983.
19. Wang, J.-H.; Yang, T.-H.; Wu, W.-W.; Chen, L.-J.; Chen, C.-H.; Chu, C.-J. *Nanotechnology* **2006**, *17*, 719.
20. Masarapu, C.; Ok, J. T.; Wei, B. *J. Phys. Chem. C* **2007**, *111*, 12112.
21. Fang, X.; Bando, Y.; Gautam, U.; Ye, C.; Golberg, D. *J. Ma-*

ter. Chem. **2008**, *18*, 509.
22. Ren, H.-X.; Huang, X.-J.; Yarimaga, O.; Choi, Y.-K.; Gu, N. *J. Colloid Interf. Sci.* **2009**, *334*, 103.
23. Li, J.; Guo, Z.; Liu, J.-H.; Huang, X.-J. *J. Phys. Chem. C* **2011**, *115*, 16934.
24. Qu, M.; Zhaol, G.; Wang, Q.; Caol, X.; Zhang, J. *Nanotechnology* **2008**, *19*, 055707.
25. Qian, B.; Shen, Z. *Langmuir* **2005**, *21*, 9007.
26. Neto, C.; Joseph, K. R.; Brant, W. R. *Phys. Chem. Chem. Phys.* **2009**, *11*, 9537.
27. Zhao, N.; Shi, F.; Wang, Z. Q.; Zhang, X. *Langmuir* **2005**, *21*, 4713.
28. Barthlott, W.; Neinhuis, C. *Planta* **1997**, *202*, 1.
29. Feng, L.; Li, S.; Li, Y.; Li, H.; Zhang, L.; Zhai, J.; Song, Y.; Liu, B.; Jiang, L.; Zhu, D. *Adv. Mater.* **2002**, *14*, 1857.
30. Gu, Z. Z.; Uetsuka, H.; Nakajima, K. R.; Onishi, H.; Fujishima, A.; Sato, O. *Angew. Chem. Int. Ed.* **2003**, *42*, 894.
31. Oner, D.; McCarthy, T. J. *Langmuir* **2000**, *16*, 7777.
32. Olde, R.; Terlingen, J. G. A.; Engbers, G. H. M.; Feijen, J. *Langmuir* **1999**, *15*, 4847.
33. Shirtcliffe, N. J.; McHale, G.; Newton, M. I.; Perry, C. C. *Langmuir* **2005**, *21*, 937.
34. Feng, X.; Jiang, L. *Adv. Mater.* **2006**, *18*, 3063.
35. Huang, T.-K.; Chen, Y.-C.; Ko, H.-C.; Huang, H.-W.; Wang, C.-H.; Lin, H.-K.; Chen, F.-R.; Kai, J.-J.; Lee, C.-Y.; Chiu, H.-T. *Langmuir* **2008**, *24*, 5647.
36. Sun, Y. G.; Mayers, B.; Herricks, T.; Xia, Y.-N. *Nano Lett.* **2003**, *3*, 955.
37. Gao, Y.; Jiang, P.; Liu, D. F.; Yuan, H. J.; Yan, X. Q.; Zhou, Z. P.; Wang, J. X.; Song, L.; Liu, L. F.; Zhou, W. Y.; Wang, G.; Wang, C. Y.; Xie, S. S.; Zhang, J. M.; Shen, D. Y. *J. Phys. Chem. B* **2004**, *108*, 12877.
38. Reyes-Gasgaa, J.; Elechiguerraa, J. L.; Liub, C.; Camacho-Bragadob, A.; Montejano-Carrizalesc, J. M.; Jose Yacamana, M. *J. Cryst. Growth* **2006**, *286*, 162.
39. Fowler, R. H.; Nordheim, L. W. *Proc. R. Soc. A* **1928**, *119*, 173.
40. Xu, J. W.; Yun, K.; Zhu, Z. *Physica E* **2010**, *42*, 1451.
41. Chang, I.-C.; Huang, T.-K.; Lin, H.-K., Tzeng, Y.-F.; Peng, C.-W.;Pan, F.-M.; Lee, C.-Y.; Chiu, H.-T. *ACS Appl. Mater. Interfaces* **2009**, *1*, 1375.
42. Cassie, A. B. D.; Baxter, S. *Trans. Faraday Soc.* **1944**, *40*, 546.

